Journal of Molecular Catalysis A: Chemical 425 (2016) 255–265

Contents lists available at ScienceDirect

Journal of Molecular Catalysis A: Chemical

journal homepage: www.elsevier.com/locate/molcata

Editor's choice paper

Effect of basicity on the catalytic properties of Ni-containing hydrotalcites in the aerobic oxidation of alcohol

Weiyou Zhou, Qianyun Tao, Jiugao Pan, Jie Liu, Junfeng Qian, Mingyang He*, Qun Chen

Jiangsu Key Laboratory of Advanced Catalytic Materials and Technology, Changzhou University, Changzhou 213164, China

ARTICLE INFO

Article history:
Received 25 July 2016
Received in revised form 12 October 2016
Accepted 16 October 2016
Available online 18 October 2016

Keywords:
Basicity
Ni-containing hydrotalcites
Magnesium
Alcohol oxidation

ABSTRACT

A series of Ni-containing hydrotalcites with different basicities have been prepared by introducing different Mg^{2+} contents, and characterized by XRD, SEM, TG-DTG, ICP, FTIR, Hammett analysis, DR UV–vis, XPS, etc. The effects of basicity on the catalytic performance in the selective aerobic oxidation of alcohols and the mechanism have been studied. The results showed that substituting Ni^{2+} in the structure by Mg^{2+} ions significantly increased the surface basicity of the catalysts. The surface basicity of Ni-containing hydrotalcites could accelerate the first acid-base reaction step in the oxidation and improve the catalytic activity. Varied alcohols were tested and discussed in the reaction system to verify the effect, and the results indicated that the activity of α-C—H bond is the key factor for the benzyl alcohol derivatives, while the first base-acid reaction step may be more important for aliphatic alcohols. The comparison results between the hydrotalcites and the calcined samples showed that the type of basic site have significantly influence on the catalytic activity, and only the Brønsted OH basic sites accelerate the oxidation. In addition, a probable mechanism for the reaction was postulated based on catalytic results, Hammett and a series of controlled experiments. The main factors affecting the catalytic oxidation of varied alcohols using molecular oxygen as the ultimate oxidant have been discussed, which may be helpful in designing more efficient catalyst.

1. Introduction

Development of efficient catalyst for the selective oxidation of alcohol to carbonyl compounds is one of the important topics in synthetic and industrial chemistry, and has attracted so much attention from chemists [1–3]. It is very difficult to control the reaction because of over oxidations or side reactions under conventional severe reaction conditions [4,5]. Therefore, many protocols have been proposed for the catalytic transformation, including direct dehydrogenation [6–8] and oxidation in the presence of various oxidant, such as *tert*-butyl hydroperoxide (TBHP) [9,10], H_2O_2 [11–13], $NaIO_4$ [14], *meta*-chloroperoxybenzoic acid (*m*CPBA) [15] and O_2 [16–20], etc.

Obviously, catalytic oxidation with molecular oxygen is particularly attractive from an economical and environmental point of view. Moreover, heterogeneous catalysts in the liquid-phase offer several advantages over homogeneous ones, such as an ease of recovery and recycling, atom utility, and enhanced stability in the oxidation reactions. Unfortunately, most of these catalytic processes using O_2 needed high pressure of oxygen, high reaction temperature or additives, including base [21–23], coreductant [24,25], NHPI [26,27] and TEMPO [28,29], etc.

It should be very interesting if molecular oxygen is activated under low temperature and atmospheric pressure without any other additives in the oxidation of alcohol. To achieve the goal, it is very important to develop a highly efficient catalyst. Actually, some heterogeneous catalysts originated from noble metals for the reaction system using O_2 as the ultimate oxidant have been developed, including Ru [30,31], Au [32–34], Pt [35] and Pd [36,37], etc. However, from the viewpoint of economy and sustainable chemistry, it is especially important to develop economically catalysts for the selective oxidation of alcohol, because noble metal catalysts are highly expensive and scarce.

To date, some catalytic systems based on the non-noble metals for the transformation of alcohol to carbonyl by molecular oxygen have been reported. Synthetic cryptomelane octahedral molecular sieve (OMS-2) with a tunnel structure has been reported as a heterogeneous catalyst in the oxidation of benzyl alcohol [38,39]. The reaction proceeded via activation of molecular oxygen through the lattice oxygen in manganese oxide associated with the Mn(IV)/Mn(II) reduction-oxidation couple. Choudary [40] and Kawabata [41] groups reported that activation of molecu-

* Corresponding author.
E-mail addresses: hemy_cczu@126.com, hmy@cczu.edu.cn (M. He).

http://dx.doi.org/10.1016/j.molcata.2016.10.017
1381-1169/

lar oxygen on nickel-containing hydrotalcite-like anionic clay also took place in the oxidation of alcohols. Li et al. [42] have found that NaOH treated VSB-5 phosphates molecular sieve possessed efficient activities in the transformation. They thought treatment by NaOH resulted in highly dispersed Ni(OH) active species. And according to their proposed mechanism, the substrate alcohol first bound to the Ni^{2+} center through interacting with basic OH^- ion, followed by hydride transfer from the alcoholate to the neighboring Ni atom to generate the carbonyl product. These results indicated that the surface basicity of the catalyst should have important effect on the catalytic performance. In our previous research, we have also found that the basicity of hydrotalcites could significantly affect their catalytic performances in the alcohol oxidation [43,44].

Hydrotalcites is a typical basic material, the properties can be fine-tuned via the adjustability of the cations and anions in the brucite layer and interlayer [45,46]. Although the Ni-containing hydrotalcite-type anionic clay catalysts have been reported in the oxidation of alcohol, the effect of the surface basicity on the catalytic performance in the transformation has not been studied. In addition, the reaction mechanism is also debatable. Choudary [40] and Kawabata [41] thought that peroxide formed in the reaction and abstracted the α-H, while in Li's catalytic system, the step was replaced by the hydride transfer from the alcoholate to Ni atom. On the other hand, CO_3^{2-} was thought to be very important in the Choudary's catalytic system, while there was no CO_3^{2-} existed in the NaOH treated VSB-5 phosphates molecular sieve. The knowledge of the basicity's function and the mechanism should be helpful in designing the economic catalysts with high catalytic performance in the aerobic oxidation of alcohol.

In the present study, therefore, a series of Ni-containing hydrotalcites (CO_3^{2-}-Ni_2Mg_xAl-LDHs, x = 0, 0.5, 1.0, 1.5, and 2.0) with different basicities have been prepared by changing the Mg^{2+} contents in the structure. And the effect of surface basicity on their catalytic properties in the selective aerobic oxidation of alcohols has been detailedly studied. In addition, the influences of the main factors including alcohol's structure on the reaction and the possible mechanism have also been discussed.

2. Experimental

2.1. Preparation of catalysts

CO_3^{2-}-Ni_2Mg_xAl LDHs with different Mg contents (x = 0, 0.5, 1.0, 1.5 and 2.0) were synthesized by a coprecipitation method. In a typical procedure, 0.04 mol of $Ni(NO_3)_2{\cdot}6H_2O$, 0.02 mol of $Mg(NO_3)_2{\cdot}6H_2O$ and 0.02 mol of $Al(NO_3)_3{\cdot}9H_2O$ were dissolved in 120 mL deionized water to form solution A, and solution B was prepared by dissolving 0.067 mol of Na_2CO_3 and 0.2 mol of NaOH in 120 mL deionized water. The two solutions were added dropwise with stirring to 120 mL deionized water at 60 °C while the pH was maintained 10.0 ± 0.5. After that, the resulting slurry was stirred for another 30 min and then digested at 80 °C for 24 h. The precipitate was washed with deionized water until the pH of the filtrate was around 7.0. And then dried in an oven at 100 °C for 12 h. The solid obtained was named CO_3^{2-}-Ni_2MgAl-LDH. The sample calcined under 300 °C for 4 h using CO_3^{2-}-Ni_2MgAl-LDH as the precursor was named Ni_2MgAl-LDO-300. Other samples with different Mg^{2+} content and calcination temperature were synthesized via similar method.

2.2. Characterization of catalysts

Powder X-ray diffraction (XRD) patterns of these prepared samples were obtained from a Rigaku D/max 2500 PC X-ray diffractometers with Cu-Kα (1.5402 Å) radiation at 10 min^{-1}. Inductively coupled plasma analysis (ICP) was used to analyze the compositions of samples in a Varian Vista-AX device. Diffuse reflectance ultraviolet visible spectra (DR UV–vis) were recorded in a Perkin-Elmer Lambda 35 spectrophotometer, using $BaSO_4$ as a reference. The IR spectra were obtained on a Nicolet PROTÉGÉ 460 FTIR spectrometer in the region 4000–400 cm^{-1} using KBr pellets. Porosity and surface area studies were performed on a micromeritics ASAP2010C apparatus, using nitrogen as the adsorbate at liquid nitrogen temperature (−196 °C). All the samples were outgassed under vacuum for 16 h at 298 K before the adsorption measurements. The surface area was calculated using the BET method and the pore size distributions were deduced from the adsorption branches of the isotherms using the BJH method. The basic properties were determined by titration with 0.01 M benzoic acid solution in toluene using 0.1 g of vacuum dried solid sample suspended in 2 mL of phenolphthalein indicator solution [47].

2.3. Reaction procedure for benzyl alcohol oxidation

Liquid-phase catalytic oxidation of benzyl alcohol was carried out in a 25 mL two-neck-flask with reflux condenser and magnetically stirred autoclave heated in an oil bath under atmospheric pressure. Dioxygen was bubbled (10 mL/min) through a solution of toluene (8 mL), benzyl alcohol (216 mg, 2 mmol), and catalyst (1.0 g) at 80 °C. The product samples were drawn at regular time intervals and analyzed with a gas chromatography (Shimadzu GC-2010AF) having SE-30 capillary column and FID detector. The products were further confirmed using GC–MS (Shimadzu GCMS-2010) with a DB-5MS capillary column. After the reaction, the resulting mixture was cooled with ice bath and the catalyst was separated by centrifugation and washed with solvent. After drying at room temperature in vacuum, the recycled catalyst can be reused in the next run under the same conditions. The conversion, yield of benzaldehyde and selectivity presented here are based on the GC calculations using chlorobenzene as the internal standard reference compound.

2.4. Competitive reactions of benzyl alcohol and para-substituted benzyl alcohols for Hammett plot

The reaction was carried out in the presence of an excess of substrate. To a mixture of benzyl alcohol (5 mmol) and *para*-(X)-substituted benzyl alcohol (5 mmol, X = —OCH_3, —CH_3, —Cl, and —NO_2), chlorobenzene (10 mmol, as the internal standard reference compound), CO_3^{2-}-Ni_2MgAl-LDH (0.5 g), and solvent toluene 8 mL was bubbled dioxygen (10 mL/min). The mixture was stirred at 80 °C and samples were drawn at regular time intervals and analyzed by GC. The relative reactivities were determined using the following equation: $k_x/k_H = C_xX_i/C_HH_i$, where C_x and X_i are the conversion and the initial concentration of benzyl alcohol, C_H and H_i are the conversions and the initial concentrations of substituted benzyl alcohols.

3. Results and discussion

3.1. Characterization of CO_3^{2-}-Ni_2Mg_xAl- LDHs samples

For the synthesis of LDHs compounds, the M^{2+}/M^{3+} ratio has significant effect on the structure. Therefore, we prepared CO_3^{2-}-Ni_2Mg_xAl-LDHs with the (Ni + Mg)/Al ratio between 2.0 to 4.0 to obtain the pure hydrotalcite compounds.

The powder XRD patterns for CO_3^{2-}-Ni_2Mg_xAl-LDHs are depicted in Fig. 1. The patterns of all the samples show characteristic LDH reflections (sharp and symmetrical for (003) and (006), broad and asymmetrical for (009), (015) and (018), respectively) [40,48,49]. Furthermore, the distinguishable reflections corresponding to planes (110) and (113) (recorded in the 2θ range

Table 1
Sample notation and chemical compositions of CO_3^{2-}-Ni_2Mg_xAl-LDHs.

Sample	Weight content (%)			Ni:Mg:Al	S_{BET} (m^2/g)	Pore volume (cm^3/g)	Pore size distribution (nm)	pH[a]	Basicity at H_- = 7.6–10.0 (mmol/g)[b]
	Ni	Al	Mg						
CO_3^{2-}-Ni_2Al-LDH	31.25	7.95	–	1.8:0:1	109	0.15	3.8	8.01	0.323
CO_3^{2-}-$Ni_2Mg_{0.5}Al$-LDH	27.17	7.23	2.99	1.7:0.5:1	105	0.26	2.8, 6.1	8.32	0.435
CO_3^{2-}-Ni_2MgAl-LDH	26.26	6.49	5.61	1.9:0.9:1	156	0.20	2.5, 5.5	8.75	0.650
CO_3^{2-}-$Ni_2Mg_{1.5}Al$-LDH	24.95	5.71	7.56	2.0:1.5:1	95	0.20	2.4, 5.5	8.97	0.912
CO_3^{2-}-Ni_2Mg_2Al-LDH	23.91	5.47	9.44	2.0:1.9:1	110	0.33	2.5, 5.5	9.05	1.151

[a] Suspension of 0.3 g hydrotalcite in 20 mL deionized water.
[b] 0.1 g hydrotalcite, suspended in 2 mL phenolphthalein indicator solution, is titrated with 0.01 M benzoic acid.

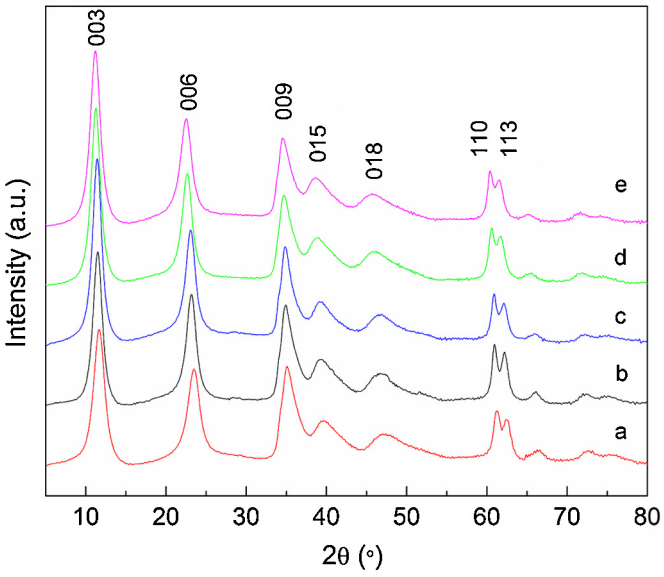

Fig. 1. XRD patterns of CO_3^{2-}-Ni_2Mg_xAl-LDHs (a) x = 0; (b) x = 0.5; (c) x = 1; (d) x = 1.5; (e) x = 2.

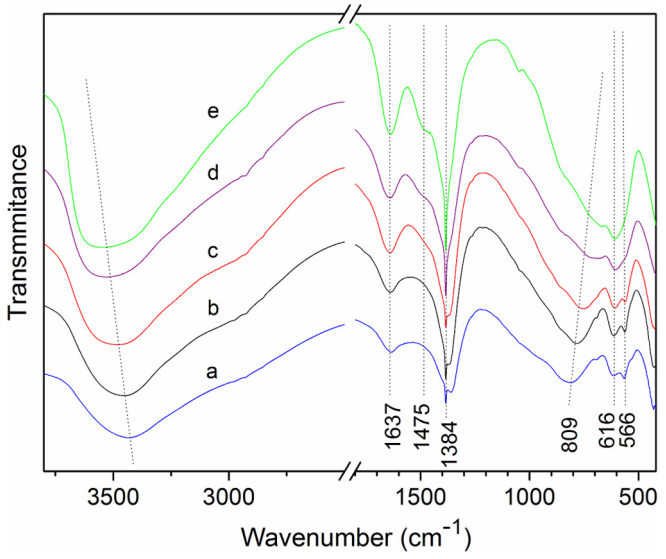

Fig. 2. FTIR spectra of CO_3^{2-}-Ni_2Mg_xAl-LDHs (a) x = 0; (b) x = 0.5; (c) x = 1; (d) x = 1.5; (e) x = 2.

60–63°) suggest a well ordering of both the anions of the interlayer and the cations in the layers [50,51]. These results indicate that Mg was incorporated into the hydrotalcite structures and the cations were well dispersed. The basal spacings (d basal) of CO_3^{2-}-Ni_2Mg_xAl-LDHs calculated from the (003) reflection are 7.65–7.87 Å, respectively, indicating that the interlayers of all LDHs are mainly CO_3^{2-} besides H_2O and OH^-. And the slight change of the value may be due to the incorporation of Mg^{2+}. All the samples showed the similar morphologies, and the SEM image of CO_3^{2-}-Ni_2MgAl-LDH (Fig. S1) shows that the sample formed plate-like agglomerated crystals, representing the character of layered materials [52,53]. The data of ICP analysis in Table 1 shows that the ratios of Ni/Mg/Al are almost identical to the theoretical value.

The IR spectra of CO_3^{2-}-Ni_2Mg_xAl-LDHs (x = 0, 0.5, 1, 1.5 and 2) are shown in Fig. 2, it can be found that all the samples show a broad and intense band between 3700 cm^{-1} and 3400 cm^{-1} centered at about 3500 cm^{-1} due to the —OH stretching vibration of layer hydroxyl groups and interlayer water molecules [51]. These bands shift to higher frequencies with increased Mg content, indicating a decrease of Me–OH bond strength [54], the shift may also be due to the increase of M^{2+}/M^{3+} ratio [55]. The absorption at 1637 cm^{-1} is assigned to the bending vibration of water, and 1384 cm^{-1} to the carbonate anion in the interlayers. In the 400–1000 cm^{-1} region there are some bands related to vibrations of cation–oxygen. The broaden appearance at 616 and 566 cm^{-1} and the shift at 809 cm^{-1} (the lattice vibration modes of Me—O in the LDH sheets) clearly indicate that introduction of Mg^{2+} into NiAl hydrotalcites resulted in a disordered cation distribution, which is also verified by the appearance of the shoulder peak at 1475 cm^{-1} [55,56].

TG/DTG curves of CO_3^{2-}-Ni_2Mg_xAl-LDHs (x = 0, 0.5, 1, 1.5 and 2) (Fig. S2) show two main stages of weight loss around (177.7–244.5 °C and 358.0–373.3 °C). The former peak corresponds to the loss of absorbed water and interlayer water, whereas the latter can be put down to the dehydration of hydroxyl groups on the brucite layers and also the loss of CO_2 from the interlayer. Based on the first stage, the temperature peaks show a decreasing trend as the Mg^{2+} content increases, while the second stages do not change a lot, indicating that the introduction of Mg^{2+} might disturb the orderly arranged gallery water [57].

For the purpose of exploring the textural parameters of the Mg^{2+} modified NiAl hydrotalcites, nitrogen sorption measurement was carried out. The N_2 adsorption-desorption isotherm at −196 °C and the corresponding pore size distribution curves for CO_3^{2-}-Ni_2Mg_xAl-LDHs with different Mg^{2+} contents were shown in Fig. 3. We can see that the isotherm for these samples are all type IV according to the IUPAC classification, conforming the mesoporous structure of the materials. On the other hand, differences in the hysteresis loops indicate different types of pore shapes which can be correlated with the different composition of the layered sheets. For the CO_3^{2-}-Ni_2Al-LDH and the samples with low Mg^{2+} contents, H2 type hysteresis loops are observed, while CO_3^{2-}-$Ni_2Mg_{1.5}Al$-LDH and CO_3^{2-}-Ni_2Mg_2Al-LDH show broad H3 type hysteresis loops, attributed to aggregates of plate-like particles containing slit-shaped pores [58].

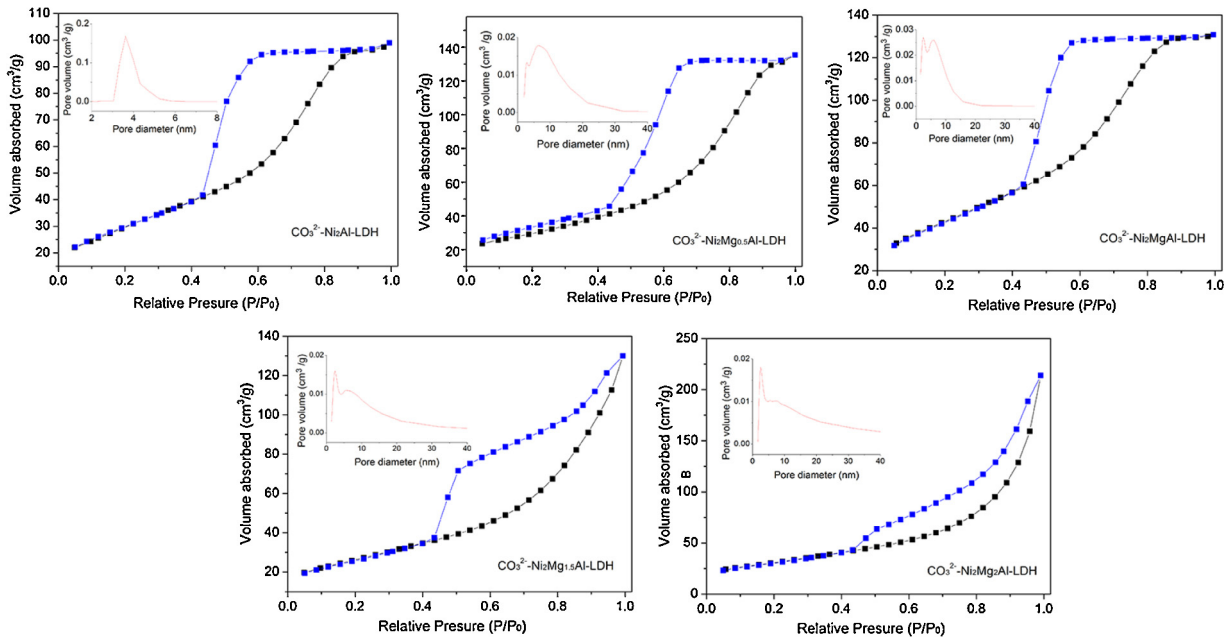

Fig. 3. N_2 adsorption/desorption isotherms and pore size distribution (inserted picture) of CO_3^{2-}-Ni_2Mg_xAl-LDHs.

The data of the surface areas, pore volumes and pore sizes of these samples are summarized in Table 1. After introducing Mg^{2+}, the BET surface area of these samples are all changed irregularly, and CO_3^{2-}-Ni_2MgAl-LDH exhibited the highest value of 156 m^2/g, markedly better than that reported in literature [41]. The pore volumes of these Mg^{2+} modified samples are all bigger than CO_3^{2-}-Ni_2Al-LDH, while the pore size distributions are widened. Upon introduction of Mg^{2+} into NiAl hydrotalcites, changes in the porosity characteristics may be attributed to the alteration of the microscopic morphology due to the presence of different cations within the structure, consistent with the previously reported results [58,59].

Temperature-programmed desorption of carbon dioxide (CO_2-TPD) is an efficient method for measuring the basicity of samples, but the high temperature needed during the pretreatment must destroy the structure of LDHs samples. Therefore, the amount of the basic sites in the catalysts was analyzed qualitatively using Hammett indicators. The results in Table 1 show that the basic strength and the total basic sites on the surface of these samples increased with the enhancement of Mg^{2+} content, indicating that changing the Mg^{2+} content is an effective method for adjusting the basicity of these samples.

DR UV–vis spectroscopy is an effective method to detect coordination states of incorporated nickel species in various materials. Fig. S3 shows the DR UV–vis spectra of the prepared CO_3^{2-}-Ni_2Mg_xAl-LDHs with different Mg^{2+} content. The spectra of all the samples are highly similar, with two split broad bands with two pairs of maxima at 741, 649 and 412, 380 nm. The results are accordance to the Kawabata's that with different Ni/Mg/Al compositions, indicating that Ni(II) is octahedrally coordinated in CO_3^{2-}-Ni_2Mg_xAl-LDHs [41,60].

The XPS spectra were also used to analyze of these prepared samples, and the Ni 2p spectra of these LDHs with different Mg content are shown in Fig. 4. All these samples show similar spectra. The Ni $2p_{3/2}$ (≈855.8 eV) an ied with two satellite bands and a spin-energy separation of about 17.6 eV further indicate the presence of Ni(II) in LDHs [61,62]. The O 1s spectra of these catalysts also showed the similar spectra of the binding energies between 531.3–531.5 eV (Fig. S4), corresponding to the Me—OH oxygen atom. These results further indicate that Mg^{2+} has been incorporated into the hydrotalcite structures and the cations were uniformly dispersed.

3.2. Oxidation of benzyl alcohol catalyzed by CO_3^{2-}-Ni_2Mg_xAl-LDHs samples

In this present investigation, the oxidation of benzyl alcohol was examined as a standard substrate catalyzed by CO_3^{2-}-Ni_2MgAl-LDH samples using molecular O_2 as the sole oxidant. The blank experiment (Table 2, entry 1) exhibited that the prepared samples performed as the catalyst in the oxidation. Before discussing the effect of basicity on the catalytic activities of these catalysts, the solvent, reaction temperature and catalyst amount have been first optimized (the main data are summarized in Table 2). All the selected solvent exhibited almost 100% selectivities of benzaldehyde, while the toluene showed the highest conversion and yield (Table 2, entries 2–8). No product was observed without benzyl alcohol as the substrate, indicating that the catalyst could not catalyze the oxidation of toluene. As to the reaction temperature, it is observed that (Table 2, entries 2, 9 and 11) low reaction temperature significantly reduced the catalytic performance, the same pattern was found in the influence of the amount of catalysts (Table 2, entries 2, 12 and 13). 1.0 g of catalyst and 80 °C were found to be enough for the transformation, although no by-product benzoic acid was observed when the temperature was increased to 90 °C. The yield of benzaldehyde reached to >99% under the optimized conditions in the catalytic system. The recycled experiments (Table 2, entries 18 and 19) showed that the prepared catalyst could be reused at least five times without changes of catalytic activity, indicating that the synthesized CO_3^{2-}-Ni_2MgAl-LDH is a stable catalyst. The XRD pattern of the recycled catalyst in Fig. S5 shows that the structure of the catalyst did not change in the catalytic oxidation.

In addition, some typical heterogeneous catalytic systems for the oxidation of benzyl alcohol using O_2 as the sole oxidant have been collected in Table 3 for comparision. To make the comparision convenient, the concept "specific activity" was used instead of TOF (turnover frequency). It can be found that non-noble metals generally show less catalytic activity than precious metal catalysts. However, CO_3^{2-}-Ni_2MgAl-LDH gave the excellent conversion and

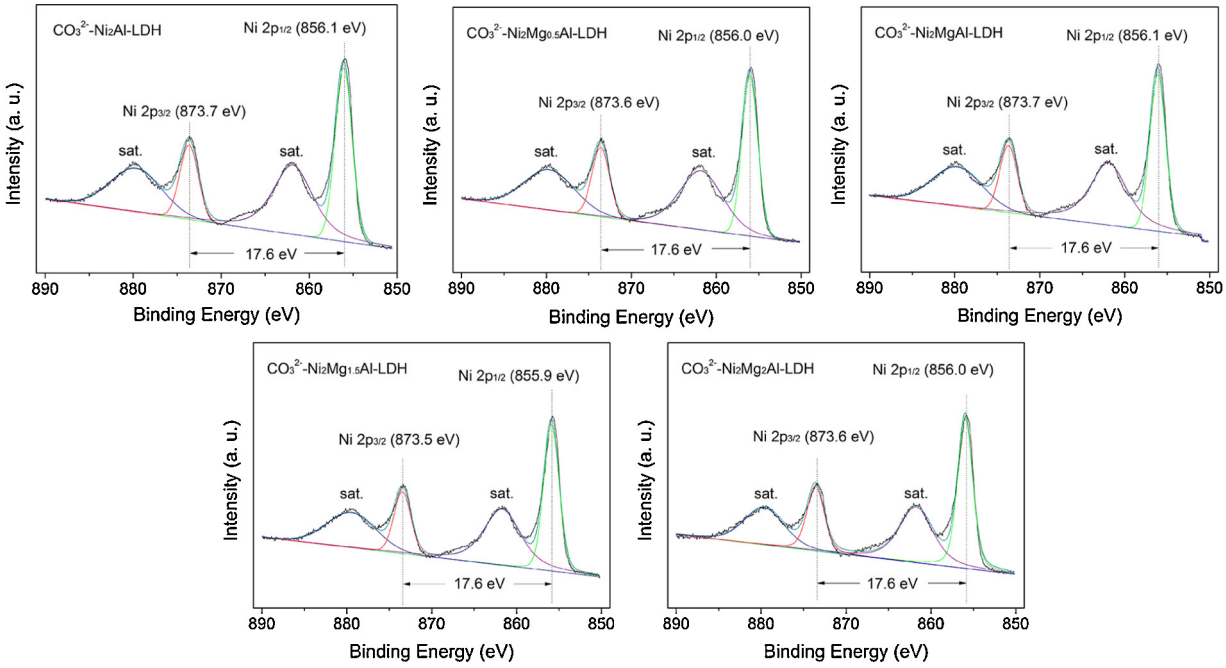

Fig. 4. XPS survey spectra of CO_3^{2-}-Ni_2Mg_xAl-LDHs (x = 0, 0.5, 1, 1.5 and 2).

Table 2
Optimization of reaction conditions.

Entry	Catalyst	Solvent	T (°C)	Amount of catalyst (g)	Conversion (%)	Selectivity of aldehyde (%)
1	No catalyst	toluene	80	–	0	–
2	CO_3^{2-}-Ni_2MgAl-LDH	toluene	80	1.0	>99	>99
3	CO_3^{2-}-Ni_2MgAl-LDH	dimethyl sulfoxide	80	1.0	28.9	>99
4	CO_3^{2-}-Ni_2MgAl-LDH	DMF	80	1.0	16.7	>99
5	CO_3^{2-}-Ni_2MgAl-LDH	cyclohexane	80	1.0	77.8	>99
6	CO_3^{2-}-Ni_2MgAl-LDH	acetonitrile	80	1.0	34.2	>99
7	CO_3^{2-}-Ni_2MgAl-LDH	1,4-dioxane	80	1.0	19.9	>99
8	CO_3^{2-}-Ni_2MgAl-LDH	ethyl acetate	80	1.0	36.8	>99
9	CO_3^{2-}-Ni_2MgAl-LDH	toluene	60	1.0	83	>99
10	CO_3^{2-}-Ni_2MgAl-LDH	toluene	70	1.0	90	>99
11	CO_3^{2-}-Ni_2MgAl-LDH	toluene	90	1.0	>99	>99
12	CO_3^{2-}-Ni_2MgAl-LDH	toluene	80	0.6	87	>99
13	CO_3^{2-}-Ni_2MgAl-LDH	toluene	80	0.8	94	>99
14	CO_3^{2-}-Ni_2Al-LDH	toluene	80	1.0	76.3	>99
15	CO_3^{2-}-$Ni_2Mg_{0.5}Al$-LDH	toluene	80	1.0	92.7	>99
16	CO_3^{2-}-$Ni_2Mg_{1.5}Al$-LDH	toluene	80	1.0	96.5	>99
17	CO_3^{2-}-Ni_2Mg_2Al-LDH	toluene	80	1.0	92.2	>99
18	CO_3^{2-}-Ni_2MgAl-LDH ^{3rd}	toluene	80	1.0	>99	>99
19	CO_3^{2-}-Ni_2MgAl-LDH ^{5th}	toluene	80	1.0	>99	>99

Reaction conditions: benzyl alcohol 2 mmol; solvent 8 mL; O_2 10 mL/min, 8 h.

Table 3
Some typical results of heterogeneous catalytic systems for the oxidation of benzyl alcohol using O_2 as the sole oxidant.[a]

Entry	Catalyst	Conversion (%)	Selectivity (%)	Specific activity[b] (mmol/g/h)	Ref.
1	CO_3^{2-}-Ni_2MgAl-LDH	>99	>99	0.25	This work
2	VSB-5 nickel phosphate	93	99.9	0.31	[42]
3	$Mg_{2.5}Ni_{0.5}Al$-HT	51.8	97.8	0.35	[41]
4	Ni_2Al-HT	31[c]		0.10	[40]
5	H-K-OMS-2	97	100	4.9	[39]
6	Au/CuO	85.7	99	0.86	[63]
7	Au nanoparticles	99[c]		33	[64]
8	$Ru(OH)_x/TiO_2$(B)	99	99	25	[31]
9	Au@20Pd/SiO_2	94	88	376	[37]
10	Au/MgCr-HT	96	>99	19.2	[32]
11	Au/MgAl-HT	85	92	0.35	[35]

[a] See the reference for the detailed structure of catalyst.
[b] Specific activity: mmol of product obtained per gram of catalyst per hour.
[c] Yield of benzaldehyde.

selectivity in the reaction with a comparable specific activity with other non-noble catalysts and some of the precious samples.

3.3. Investigation of the basicity's function in the aerobic oxidation of alcohol by CO_3^{2-}-Ni_2Mg_xAl-LDHs

3.3.1. Effect of Mg^{2+} on the catalytic activity

Under the selected conditions, the effect of Mg^{2+} on the catalytic performance was then discussed. The results in Table 2 show that these CO_3^{2-}-Ni_2Mg_xAl-LDHs samples could smoothly catalyze the aerobic oxidation of benzyl alcohol with benzaldehyde as the only product. Introduction of Mg^{2+} into the NiAl hydrotalcites exhibits a significant influence on the catalytic performance (Table 2, entries 2, 14–17). Comparing CO_3^{2-}-Ni_2MgAl-LDH with CO_3^{2-}-Ni_2Al-LDH, the conversion of benzyl alcohol significantly increased from 76.3% to >99%, indicating that Mg^{2+} in the structure could efficiently improve the catalytic activity. This phenomenon should be related to the changes of LDHs' properties, including S_{BET}, pore volume, pore size, surface basicity, etc. Concerning the ratio of Ni/Mg, we found that the activity reached the highest when the ratio was 2. Comparing the properties of these samples, the high activity might be first ascribed to the high S_{BET}. And the decrease of the activity of CO_3^{2-}-$Ni_2Mg_{1.5}Al$-LDH and CO_3^{2-}-Ni_2Mg_2Al-LDH might be due to the reducing of Ni content caused by the increase of Mg^{2+}.

When comparing CO_3^{2-}-Ni_2Al-LDH with CO_3^{2-}-Ni_2Mg_2Al-LDH with similar S_{BET}, we can conclude that surface basicity of catalyst is helpful for the catalytic activity, because the basic OH site on the surface first react with hydroxyl of alcohol [42]. Generally, there are some different types of OH in the structure of CO_3^{2-}-Ni_2MgAl-LDH catalyst, respectively links to Ni, Mg and Al atom. Therefore, we speculate that the basicity of the OH linked to Mg is stronger than that to Ni and Al for the different electronegativity, and the OH linked to Mg should exhibit higher activity in the reaction with alcohol. If not, introduction of Mg should decrease the catalytic activity, because the Ni concentration decreased. All the prepared samples have been further investigated with the same Ni amount in the oxidation of benzyl alcohol to elucidate the effect clearly, and the amounts of catalyst were based on 0.5 g of CO_3^{2-}-Ni_2Al-LDH. It can be obviously observed that the conversion of alcohol increases markedly as the Mg^{2+} content increase (Fig. 5).

To further validate the effect, controlled experiments using CO_3^{2-}-Ni_2Al-LDH with K_2CO_3 and KOH (the amount were calculated based on the amount of basic site of CO_3^{2-}-Ni_2MgAl-LDH) as the catalysts have been performed. The conversion of benzyl alcohol were 77.3% and 76.8%, respectively (Table 4, entries 1 and 2), nearly the same as that without base (Table 2, entry 4), indicating that the additive base in the studied system could not affect the catalytic activity, in contrast to the P123-stabilized Au-Ag alloy nanoparticles system [33]. The results also show that the added carbonate anion cannot accelerate the reaction, in contrast to the results observed by Choudary [40]. Concerning the results in Fig. 5, we suppose that only the basic sites in the structure benefit the catalytic performance, which will be further discussed combining the supposed mechanism.

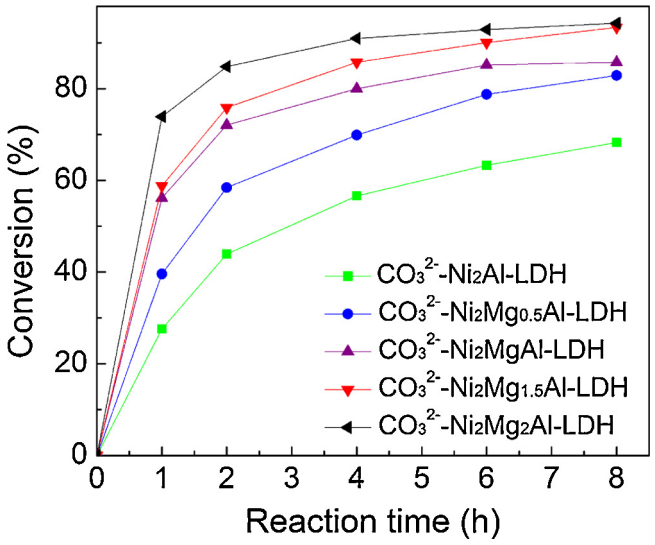

Fig. 5. Conversions of benzyl alcohol versus reaction time over different catalysts. Reaction conditions: CO_3^{2-}-Ni_2Al-LDH 0.5 g, CO_3^{2-}-$Ni_2Mg_{0.5}Al$-LDH 0.577 g, CO_3^{2-}-Ni_2MgAl-LDH 0.598 g, CO_3^{2-}-$Ni_2Mg_{1.5}Al$-LDH 0.629 g, CO_3^{2-}-Ni_2Mg_2Al-LDH 0.657 g, benzyl alcohol 2 mmol, 80 °C, toluene 8 mL, O_2 10 mL/min.

3.3.2. Effect of alcohols' structure on the transformation

To further elucidate the effect of surface basicity on the catalytic performance and the scope, various alcohols have been introduced into the reaction system. In general, when benzyl alcohol and its analogs were used as the substrates, the excellent yields were obtained (Table 5, entries 1–7) without any byproducts, which are more excellent than the reported results [40,41]. From the reaction time needed for these substrates with different substituents, it is easy to conclude that electronic variation on the aromatic substituents has some effects on the activity. Generally, benzyl alcohols substituted with electron-donating groups such as CH_3, and OCH_3 (Table 5, entries 1, 4–6) exhibited higher activity as compared to those with electron-withdrawing groups (Table 5, entries 2 and 3). An interesting result was found that the catalyst did not show any catalytic activity for the 4-hydroxybenzyl alcohol (entry 8), which should be related to the existence of the phenol hydroxyl (the reason will be discussed in the mechanism segment).

Table 4
The performance of different catalytic system in the oxidation of benzyl alcohol.[a]

Entry	Catalyst	Conversion (%)	Selectivity of aldehyde (%)
1	CO_3^{2-}-Ni_2Al-LDH + K_2CO_3[b]	77.3	>99
2	CO_3^{2-}-Ni_2Al-LDH + KOH[c]	76.8	>99
3	CO_3^{2-}-Ni_2Al-LDH[d]	11.8	>99
4	CO_3^{2-}-Ni_2MgAl-LDH[d]	54.7	>99
5	CO_3^{2-}-Ni_2MgAl-LDH[e]	61.4	>99
6	CO_3^{2-}-Ni_2MgAl-LDH[f]	>99	>99
7	CO_3^{2-}-Ni_2MgAl-LDH[g]	<5	>99

[a] Reaction conditions: benzyl alcohol 2 mmol, toluene 8 mL, catalyst 1.0 g, O_2 10 mL/min, 8 h.
[b] CO_3^{2-}-Ni_2Al-LDH 1.0 g; K_2CO_3 22.6 mg.
[c] CO_3^{2-}-Ni_2Al-LDH 1.0 g, KOH 18.3 mg.
[d] The reaction were performed under N_2 atmosphere.
[e] Same conditions were used except that the free radical inhibitor BHT (2 mmol) was added.
[f] TEMPO (2 mmol) was added.
[g] 3-Chlorophenol (2 mmol) was added.

Table 5
Catalytic oxidation of varied alcohols under CO_3^{2-}-Ni_2MgAl-LDH.[a]

Entry	Substrate	Product	Conversion (%)	Time (h)
1	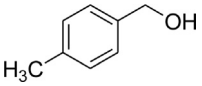	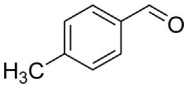	>99	4
2	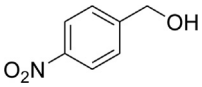	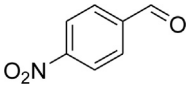	>99	4
3	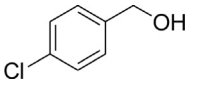	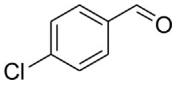	93.1	9
4	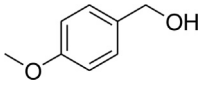	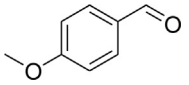	>99	4
5	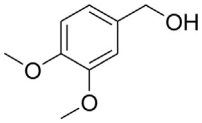	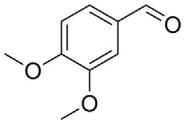	>99	2
6	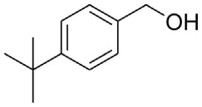	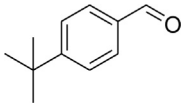	>99	6
7	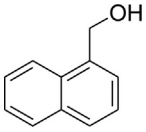	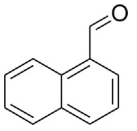	98.5	8
8	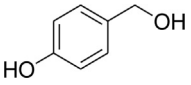	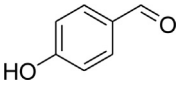	0	10
9	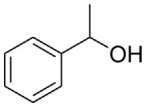	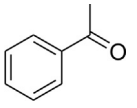	>99	8
10	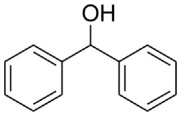	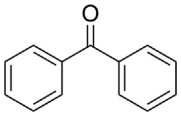	>99	2
11	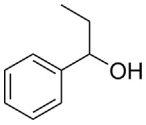	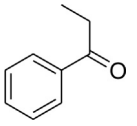	95.8	12
12	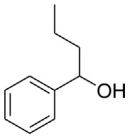	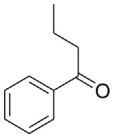	61.8	12
13	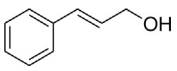	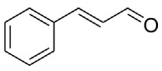	>99	6
14	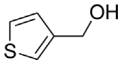	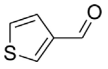	>99	4
15	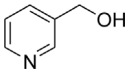	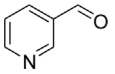	92.4	18
16	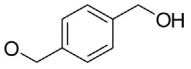	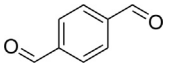	60.9	8

Table 5 (*Continued*)

Entry	Substrate	Product	Conversion (%)	Time (h)
17	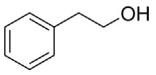	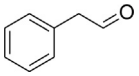	5.5 (0.5%)[b]	6
18	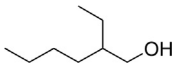	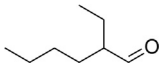	9.2 (trace)[b]	12
19	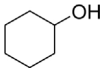		12.5 (1%)[b]	16

[a] Reaction conditions: CO_3^{2-}-Ni_2MgAl-LDH 1.0 g, substrate 2 mmol, 80 °C, toluene 8 mL, O_2 10 mL/min.
[b] Under the catalysis of CO_3^{2-}-Ni_2Al-LDH.

Table 6
The basicity of Ni_2MgAl-LDO calcined under different temperatures.

Calcination temperature (°C)	pH[a]	Basicity at H_- = 7.6–15.0 (mmol/g)[b]
300	10.65	1.62
400	10.44	1.58
500	10.42	1.50

[a] Suspension of 0.3 g hydrotalcite in 20 mL deionized water.
[b] 0.1 g hydrotalcite, suspended in 2 mL phenolphthalein indicator solution, is titrated with 0.01 M benzoic acid.

On the other hand, the oxidation of secondary alcohol could also lead to the corresponding ketone in excellent yields (Table 5, entries 9–12). 1-phenyl ethanol, 1-phenyl propanol and 1-phenyl butanol was transferred to corresponding ketone smoothly in the system, significantly higher than that under the NaOH treated VBS-5 [42], which may be related to the small pore size of the material (1.0 nm). By contrast, after the introduction of Mg^{2+}, the data for our catalysts have a widened distribution (Table 2), which could provide sufficient space for the substrates to approach the active center. On the other hand, from the results for the secondary alcohol with different carbons, it can be concluded that the steric effect also exist in the catalytic system. Good to excellent yield for the aromatic alcohols with hetero atoms (Table 5, entries 14 and 15) and diol (Table 5, entry 16) were also obtained using the catalyst.

Further, we checked the applicability for the aerobic oxidation of aliphatic alcohols (Table 5, entries 17–19), which have not been investigated in the aerobic oxidation by Ni-containing catalytic systems [40–42]. Although considerable catalytic activity for these substrates were not observed, the catalyst exhibited significantly more efficient performance than CO_3^{2-}-Ni_2Al-LDH, further indicating that introduction of Mg can improve the catalytic activity. The observation may offer a mentality for designing more efficient catalyst.

In summary, the CO_3^{2-}-Ni_2MgAl-LDH exhibited high catalytic activity for the oxidation of varied alcohols. And the structure of alcohol has a significant influence on the reaction activity.

3.3.3. *Effect of calcination on the catalytic activity*

For the hydrotalcites compounds, calcination is also an efficient method to adjust their surface basicity. To further study the effect of basicity on the catalytic performance, we calcined the CO_3^{2-}-Ni_2MgAl-LDHs under different temperatures to obtain the catalysts with different basicities. The XRD patterns in Fig. S6 of these calcined samples show that the metal oxide (Ni_2MgAl-LDO) formed when the temperature was higher than 300 °C, in according to the results reported in literatures [65,66].

To compare with the precursors easily, the amount of the basic sites in the LDO samples were also analyzed qualitatively using Hammett method. The results in Table 6 show that the basic strength and the total basic sites markedly increased after the calcination, while the differences among these samples calcined at different temperatures are not marked. After calcination, the basic site (OH^- groups) probably changed, including metal-oxygen pairs, such as Mg—O, Ni—O and Al—O, and low-coordinated oxygen atoms (O_2^- ions) [67,68]. Interestingly, their catalytic activities in the aerobic oxidation of alcohols significantly decreased (Fig. 6), indicating that the reaction is affected not only by the basicity of the catalyst, but also the type of the basic site.

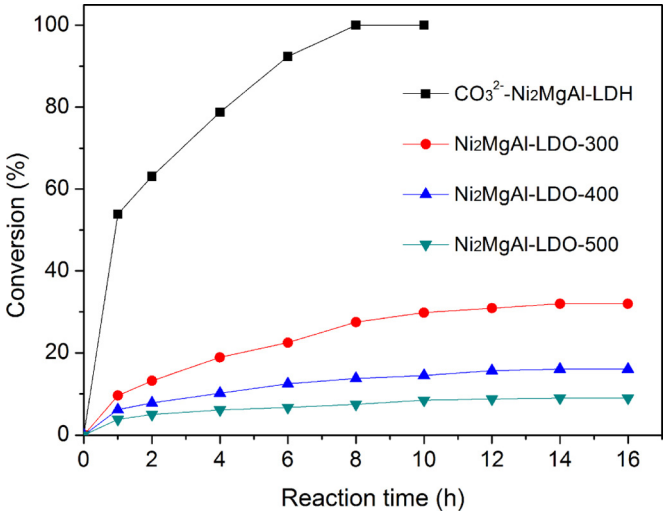

Fig. 6. Conversions of benzyl alcohol versus reaction time over Ni_2MgAl-LDO calcined under different termperatures.
Reaction conditions: benzyl alcohol 2 mmol, 80 °C, catalyst 1 g, toluene 8 mL, O_2 10 mL/min.

3.4. *Discussion of the mechanism of aerobic oxidation of alcohol under the catalysis of NiMgAl hydrotalcites*

Based on the above discussion, the reaction path of the aerobic oxidation of alcohol will be discussed in this segment. To verify if there is radical formed in the aerobic oxidation of alcohol under CO_3^{2-}-Ni_2MgAl-LDH, radical scavengers (BHT and TEMPO) were introduced into the reaction, respectively. The results (Table 4, entries 5 and 6) show that TEMPO had no effect on the reaction, while the conversion decreased to 61.4% in the presence of BHT. Then 3-chlorophenol, having stronger acidity than BHT, was investigated as the additive. A <5% conversion was observed (Table 4, entry 7), indicating that the reduction of conversion was due to the acidity of additives. The acidic additive neutralized the some basic sites of catalyst and decreased the activity. These results show that no radical formed during the reaction. Generally, the important reaction steps in alcohol dehydrogenation mainly involve cleavage of O—H and α-C—H bonds. Liu's [69] research on the Au/Cr-HT

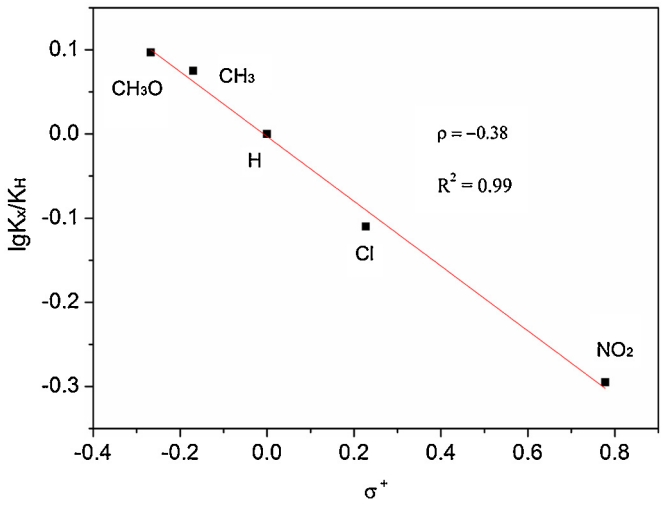

Fig. 7. Hammett plot of *p*-substituted benzyl alcohols.
Reaction conditions: 5 mmol *p*-X-benzyl alcohol (X = CH_3O, CH_3, H, Cl, NO_2), 5 mmol benzyl alcohol, CO_3^{2-}-Ni_2MgAl-LDH 0.5 g, toluene 8 mL, 1 mmol chlorobenzene, 80 °C, O_2 10 mL/min.

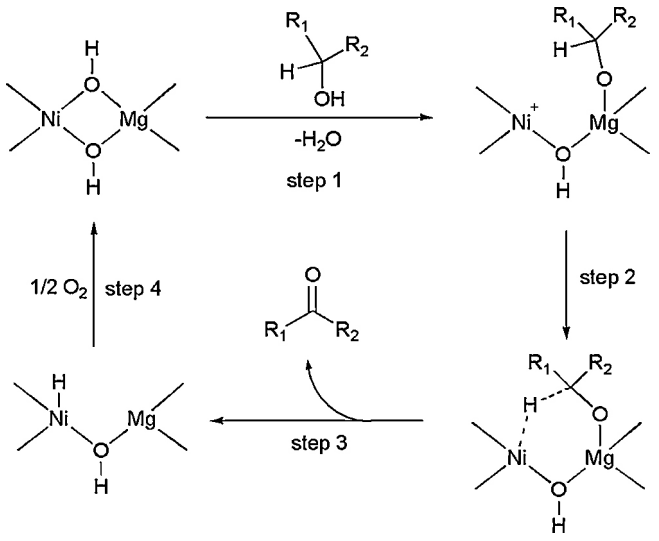

Scheme 1. The proposed mechanism of the aerobic oxidation of alcohol under CO_3^{2-}-Ni_2MgAl-LDH.

catalysts showed that both O—H and α-C—H bond cleavages are kinetically-relevant steps in alcohol oxidation.

For the cleavage of O—H, the basicity of catalyst is apparently very important, that's why introducing Mg^{2+} can improve the catalytic activity of NiAl hydrotalcites. In opposite, for the given catalyst, alcohols having different acidities should exhibit different activities in the oxidation, because the acidity of substrate affects its accessibility to the basic sites. Therefore, the low activities of aliphatic alcohols should be ascribed to their weak acidity. In a controlled experiment, benzyl alcohol and cyclohexanol (lower OH acidity than benzyl alcohol) were introduced into the reaction under N_2 atmosphere using CO_3^{2-}-Ni_2MgAl-LDH as the catalyst. After 0.5 h, the conversion of benzyl alcohol reached15.8%, markedly higher than that of cyclohexanol (5.1%), indicating the first acid-base reaction is significantly important for the transformation. In addition, compared with CO_3^{2-}-Ni_2MgAl-LDH, only a 1% conversion of cyclohexanol was obtained under CO_3^{2-}-Ni_2Al-LDH, further verified the above analysis. The same results were observed in other two kinds of alcohols (Table 5, entries 17 and 18) [70].

On the other hand, for the cleavage α-C—H bonds, a Hammett experiment has always been performed [42]. A similar test of competitive oxidations of para-substituted benzyl alcohols (X = CH_3O, CH_3, H, Cl, NO_2), which have sufficient acidic strength to react with surface basic sites, have also been conducted under the catalysis of CO_3^{2-}-Ni_2MgAl-LDH. In the competitive reaction, a large excess of substrate was used to ensure that the rate is zero order in substrate. The relative rates can be determined by the conversions of benzyl alcohol when conversions are low (<5%). The Hammett plot is shown in Fig. 7, and the slope of the Hammett plot ($\rho \approx -0.38$) was lower than that of NaOH-treated VSB-5 ($\rho \approx -0.93$). The accelerating effect of electron-donating substituents and the decelerating effect of electron-withdrawing substituents indicated that the dehydrogenation step (β-hydride elimination) is rate-limiting and the reaction is kinetically controlled [71].

In discussion of the reaction mechanism, after the formation of alcoholate species, there are two possible paths proposed in literatures for the production of carbonyl compound. One contains peroxide formed with Ni (Ni—OOH) [40,41], which abstracts α-H to form the product; and in the other path, the cleavage of α-C—H bond is facilitated by vacant coordination site of metal atom [42]. To distinguish them, we thought that a key issue was that whether the molecular oxygen participates in the single-cycle formation of carbonyl compound. Therefore, the reactions were conducted under CO_3^{2-}-Ni_2Al-LDH and CO_3^{2-}-Ni_2MgAl-LDH, respectively, without oxygen (replaced by nitrogen). The results (Table 4, entries 3 and 4) show that the yield of aldehyde reached 11.8% under CO_3^{2-}-Ni_2Al-LDH, while an interesting yield of 54.7% with CO_3^{2-}-Ni_2MgAl-LDH was obtained after 6 h. These results strongly proved that external oxygen was not necessary in the single cycle production of carbonyl compound, which is very different from that proposed by Choudhary [40] and Kawabata [41] for the Ni-containing hydrotalcites. On the other hand, comparing with the results under oxygen, the differences of the change range of conversion might be ascribed to the different catalytic activities of the two samples. The results further verify that introduction of Mg into the NiAl hydrotalcite can improve the catalytic activity in the aerobic oxidation of alcohol.

According to the reported [42] and our results, a possible catalytic reaction route for the oxidation of alcohol has been proposed (Scheme 1). Alcoholate species form through the substrate alcohol interacting with Brønsted OH group (basic site) bound to the Mg^{2+} center (step 1) present in CO_3^{2-}-Ni_2MgAl hydrotalcite. Then hydride transfers from the alcoholate to the neighboring Ni atom (step 2), simultaneously generates the carbonyl product and gives the nickel hydride species (step 3). Finally the nickel hydride species reacts with adsorbed molecular oxygen to regenerate the OH group and complete the catalytic cycle (step 4). Li et al. [42] thought that the vacant coordination site on the neighboring Ni atom site may facilitate the hydride transfer to form the carbonyl product (step 3). And in the present catalyst, the Mg atom having weaker electronegativity ($\chi_{Mg} = 1.3$, $\chi_{Ni} = 1.9$) may increase the electronic density of O atom and present higher activity than Ni.

Based on the proposed catalytic mechanism, it is easy to elucidate the less reactivity of 4-hydroxybenzyl alcohol in the catalytic system, the reason should be due to the different acidic strength of the phenol hydroxyl and alcohol hydroxyl. Because the acidity of phenol hydroxyl is stronger than alcohol, the phenol hydroxyl would first react with the basic sites on the surface of hydrotalcite and anchor the molecule, hindering the further reaction of alcohol hydroxyl with the catalysts. The above results can also provide the elucidation for the high selectivity of aldehyde, because the aldehyde molecule cannot be activated under the catalytic conditions. On the other hand, although the Lewis basic sites formed after calcination can also react with alcohol to complete the first step,

we supposed that the vacant coordination site of Ni atom cannot facilitate the split of α-C—H bond for the distance reason.

Combining the oxidation results of different substrates and the above discussion, it may be concluded that, in the aerobic oxidation under the catalysis of Ni-containing hydrotalcites, the activity of α-C—H bond is the key factor for the benzyl alcohol derivatives. However, the more important problem to be solved in the oxidation of aliphatic alcohol is improving the first base-acid reaction step.

4. Conclusions

Developing an efficient heterogeneous catalyst for the selective oxidation of alcohols using molecular oxygen as the ultimate oxidant without additives has been an important topic in the research field. In this study, NiMgAl hydrotalcites with various basicities were prepared by introducing different Mg^{2+} contents. The effect of basicity on the catalytic performance of these samples in the selective aerobic oxidation of alcohol has been essentially studied. The results showed that introduction of Mg^{2+} into NiAl hydrotalcites could efficiently adjust their surface basicities and improve the catalytic activities. The further study indicated that the type of basic sites in the structure also has important influence on the catalytic activity, and only the Brønsted OH basic sites benefit to the reaction. A probable mechanism, mainly including base-acid reaction and hydride transfer steps, was proposed based on the results. The alcohol's structure has effect on the catalytic transformation under the catalysis of NiMgAl hydrotalcites, and the activity of α-C—H bond is the key factor for the benzyl alcohol derivatives, while in the oxidation of aliphatic alcohol, the first base-acid reaction step may be more important. The study may be helpful in designing the more efficient catalysts, which can be conveniently prepared and applied in large scale.

Acknowledgments

This work was supported by Advanced Catalysis and Green Manufacturing Collaborative Innovation Center of Changzhou University, National Science Foundation of China (21403018) and Prospective Joint Research Project on the Industry, Education and Research of Jiangsu Province (BY2015027-16).

Appendix A. Supplementary data

Supplementary data associated with this article can be found, in the online version, at http://dx.doi.org/10.1016/j.molcata.2016.10.017.

References

[1] N. Gunasekaran, Adv. Synth. Catal. 357 (2015) 1990–2010.
[2] T. Mallat, A. Baiker, Chem. Rev. 104 (2004) 3037–3058.
[3] R.A. Sheldon, Catal. Today 247 (2015) 4–13.
[4] L. Delaude, P. Laszlo, J. Org. Chem. 61 (1996) 6360–6370.
[5] D.G. Lee, U.A. Spitzer, J. Org. Chem. 35 (1970) 3589–3590.
[6] A. Taketoshia, X.N. Beha, J. Kuwabaraa, T. Koizumib, T. Kanbara, Tetrahedron Lett. 53 (2012) 3573–3576.
[7] F. Wang, R.J. Shi, Z.Q. Liu, P.J. Shang, X.Y. Pang, S. Shen, Z.C. Feng, C. Li, W.J. Shen, ACS Catal. 3 (2013) 890–894.
[8] J. Yi, J.T. Miller, D.Y. Zemlyanov, R.H. Zhang, P.J. Dietrich, F.H. Ribeiro, S. Suslov, M.M. Abu-Omar, Angew. Chem. Int. Ed. 53 (2014) 833–836.
[9] S. Narayanana, J.J. Vijaya, S. Sivasanker, M. Alam, P. Tamizhdurai, L.J. Kennedy, Polyhedron 89 (2015) 289–296.
[10] B.M. Peterson, M.E. Herried, R.L. Neve, R.W. McGaff, Dalton Trans. 43 (2014) 17899–17903.
[11] S. Nojima, K. Kamata, K. Suzuki, K. Yamaguchi, N. Mizuno, ChemCatChem 7 (2015) 1097–1104.
[12] D. Shen, C.X. Miao, D.Q. Xu, C.G. Xia, W. Sun, Org. Lett. 17 (2015) 54–57.
[13] Z.P. Ye, Z.H. Fu, S. Zhong, F. Xie, X.P. Zhou, F.L. Liu, D.L. Yin, J. Catal. 261 (2009) 110–115.
[14] S. Srivastava, S. Srivastava, S. Singh, Asian J. Chem. 20 (2008) 4773–4780.
[15] J.H. Han, S.K. Yoo, J.S. Seo, S.J. Hong, S.K. Kimb, C. Kim, Dalton Trans. 2 (2005) 402–406.
[16] L.Y. Chen, H.R. Chen, R. Luque, Y.G. Li, Chem. Sci. 5 (2014) 3708–3714.
[17] M.L. Kantam, R. Arundhathi, P.R. Likhar, D. Damodara, Adv. Synth. Catal. 351 (2009) 2633–2637.
[18] Y.X. Li, Y. Gao, C. Yang, Chem. Commun. 51 (2015) 7721–7724.
[19] K. Yamaguchi, N. Mizuno, Angew. Chem. Int. Ed. 41 (2002) 4538–4542.
[20] B.M. Trost, Angew. Chem. Int. Ed. 34 (1995) 259–281.
[21] H. Tsunoyama, N. Ichikuni, H. Sakurai, T. Tsukuda, J. Am. Chem. Soc. 131 (2009) 7086–7093.
[22] H. Miyamura, R. Matsubara, Y. Miyazaki, S. Kabayashi, Angew. Chem. Int. Ed. 119 (2007) 4229–4232.
[23] C. Lavenn, A. Demessence, A. Tuel, J. Catal. 322 (2015) 130–138.
[24] C.N. Kato, M. Ono, T. Hino, T. Ohmura, W. Mori, Catal. Commun. 7 (2006) 673–677.
[25] H.B. Ji, Q.L. Yuan, X.T. Zhou, L.X. Pei, L.F. Wang, Bioorg. Med. Chem. Lett. 17 (2007) 6364–6368.
[26] M. Jafarpour, A. Rezaeifard, V. Yasinzadeh, H. Kargar, RSC Adv. 5 (2015) 38460–38469.
[27] P.J. Figiel, J.M. Sobczak, J. Catal. 263 (2009) 167–172.
[28] Z.G. Wang, Y. Jin, X.H. Cao, M. Lu, New J. Chem. 38 (2014) 4149–4154.
[29] H. Sand, R. Weberskirch, RSC Adv. 5 (2015) 38235–38242.
[30] K. Layek, H. Maheswaran, R. Arundhathi, M.L. Kantam, S.K. Bhargava, Adv. Synth. Catal. 353 (2011) 606–616.
[31] K. Yamaguchi, J.W. Kim, J.L. He, N. Mizuno, J. Catal. 268 (2009) 343–349.
[32] P. Liu, Y. Guan, R.A. Van Santen, C. Li, E.J.M. Hensen, Chem. Commun. 47 (2011) 11540–11542.
[33] X.M. Huang, X.G. Wang, X.S. Wang, X.X. Wang, M.W. Tan, W.Z. Ding, X.G. Lu, J. Catal. 301 (2013) 217–226.
[34] A. Noujima, T. Mitsudome, T. Mizugaki, K. Jitsukawa, K. Kaneda, Angew. Chem. Int. Ed. 50 (2011) 2986–2989.
[35] T. Mitsudome, A. Noujima, T. Mizugaki, K. Jitsukawa, K. Kaneda, Adv. Synth. Catal. 351 (2009) 1890–1896.
[36] Y.M.A. Yamada, T. Arakawa, H. Hocke, Y. Uozumi, Chem. Asian J. 4 (2009) 1092–1098.
[37] H.W. Wang, C.L. Wang, H. Yan, H. Yi, J.L. Lu, J. Catal. 324 (2015) 59–68.
[38] V.D. Makwana, Y.C. Son, A.R. Howell, S.L. Suib, J. Catal. 210 (2002) 46–52.
[39] Y.C. Son, V.D. Makwana, A.R. Howell, S.L. Suib, Angew. Chem. Int. Ed. 113 (2001) 4410–4414.
[40] B.M. Choudhary, M.L. Kantam, A. Rahman, C.V. Reddy, K.K. Rao, Angew. Chem. Int. Ed. 40 (2001) 763–766.
[41] T. Kawabata, Y. Shinozuka, Y. Ohishi, T. Shishido, K. Takaki, K. Takehira, J. Mol. Catal. A: Chem. 236 (2005) 206–215.
[42] C.L. Li, H. Kawada, X.Y. Sun, H.Y. Xu, Y. Yoneyama, N. Tsubaki, ChemCatChem 3 (2011) 684–689.
[43] W.Y. Zhou, J. Liu, J.G. Pan, F.A. Sun, M.Y. He, Q. Chen, Catal. Commun. 69 (2015) 1–4.
[44] W.Y. Zhou, P. Tian, F.A. Sun, M.Y. He, Q. Chen, J. Catal. 335 (2016) 105–116.
[45] Z. Wang, P. Fongarland, G.Z. Lu, N. Essayem, J. Catal. 318 (2014) 108–118.
[46] D.P. Debecker, E.M. Gaigneaux, G. Busca, Chem. Eur. J. 15 (2009) 3920–3935.
[47] R. Zăvoianu, R. Bîrjega, O.D. Pavel, A. Cruceanu, M. Alifanti, Appl. Catal. A: Chem. 286 (2005) 211–220.
[48] Z.Y. Sun, C.G. Lin, J.Y. Zheng, L. Wang, J.W. Zhang, F.L. Xu, J. Hou, Mater. Lett. 113 (2013) 83–86.
[49] A. Romero, M. Jobbígy, M. Laborde, G. Baronetti, N. Amadeo, Catal. Today 149 (2010) 407–412.
[50] P. Benito, F.M. Labajos, V. Rives, J. Solid State Chem. 179 (2006) 3784–3797.
[51] L.L. Wang, B. Li, Z.Q. Hu, J.J. Cao, Appl. Clay Sci. 72 (2013) 138–146.
[52] S. Abelló, F. Medina, D. Tichit, J. Pérez-Ramírez, X. Rodrígueza, J.E. Sueirasa, P. Salagrea, Y. Cesterosa, Appl. Catal. A: Gen. 281 (2005) 191–198.
[53] H.C. Greenwell, P.J. Holliman, W. Jones, B.V. Velasco, Catal. Today 114 (2006) 397–402.
[54] N.V. Kosova, E.T. Devyatkina, V.V. Kaichev, J. Power Sources 174 (2007) 735–740.
[55] M.J. Hernandez-Moreno, M.A. Ulibarri, J.L. Rendon, C.J. Serna, Phys. Chem. Miner. 12 (1985) 34–38.
[56] G. Carja, L. Dartu, K. Okada, E. Fortunato, Chem. Eng. J. 222 (2013) 60–66.
[57] C. Zhang, S.G. Yang, H.Z. Chen, H. He, C. Sun, Appl. Surf. Sci. 301 (2014) 329–337.
[58] E.M. Seftel, M. Niarchos, N. Vordos, J.W. Nolan, M. Mertens, A.Ch. Mitropoulos, E.F. Vansant, Microporous Mesoporous Mater. 203 (2015) 208–215.
[59] E.M. Seftel, E. Popovici, M. Mertens, G. Van Tendeloo, P. Cool, E.F. Vansant, Microporous Mesoporous Mater. 111 (2008) 12–17.
[60] P. Kim, Y. Kim, H. Kim, I.K. Song, J. Yi, Appl. Catal. A: Gen. 272 (2004) 157–166.
[61] J. Zhao, J. Chen, S. Xu, M. Shao, Q. Zhang, F. Wei, J. Ma, M. Wei, D.G. Evans, X. Duan, Adv. Funct. Mater. 24 (2014) 2938–2946.
[62] M. Li, F. Liu, J.P. Cheng, J. Ying, X.B. Zhang, J. Alloy. Compd. 635 (2015) 225–232.
[63] H. Wang, W.B. Fan, Y. He, J.G. Wang, J.N. Kondo, T. Tatsumi, J. Catal. 299 (2013) 10–19.
[64] Z.J. Huang, F.B. Li, B.F. Chen, G.Q. Yuan, Green Chem. 17 (2015) 2325–2329.
[65] P.J. Tan, Z.H. Gao, C.F. Shen, Y.L. Du, X.D. Li, W. Huang, Chin. J. Catal. 35 (2014) 1955–1971.
[66] Q. Zhao, S.L. Tian, L.X. Yan, Q.L. Zhang, P. Ning, J. Hazard. Mater. 285 (2015) 250–258.
[67] P. Liu, M. Derchi, E.J.M. Hensen, Appl. Catal. B: Environ. 144 (2014) 135–143.

[68] D.F. Wang, X.L. Zhang, C.L. Liu, T.T. Cheng, W. Wei, Y.H. Sun, Appl. Catal. A: Gen. 505 (2015) 478–486.
[69] P. Liu, V. Degirmenci, E.J.M. Hensen, J. Catal. 313 (2014) 80–91.
[70] We have ever tried to verify the acid-base reaction step using ^{18}O labeled benzyl alcohol as the substrate. But the H_2O exists in the catalyst and forms in the reaction can influence the ^{16}O and ^{18}O abundances in the product, because aldehyde and H_2O can exchange the O atom during the reaction.
[71] J.A. Mueller, C.P. Goller, M.S. Sigman, J. Am. Chem. Soc. 126 (2004) 9724–9734.